

Use of middle infrared radiation to estimate the leaf area index of a boreal forest

DOREEN S. BOYD,¹ TOBY E. WICKS² and PAUL J. CURRAN²

¹ Centre for Earth and Environmental Science Research, School of Geography, Kingston University, Penryhn Road, Kingston-upon-Thames, Surrey KT1 2EE, U.K.

² Department of Geography, University of Southampton, Highfield, Southampton, Hampshire SO17 1BJ, U.K.

Received June 3, 1999

Summary The leaf area index (LAI) of boreal forest can be estimated using reflected radiation recorded by satellite sensors. Measurements of visible and near infrared radiation are commonly used in the normalized difference vegetation index (NDVI) to estimate LAI. However, research, mainly in tropical forest, has demonstrated that LAI is related more closely to radiation of middle infrared wavelengths than of visible wavelengths. This paper derives a vegetation index, VI3, based on radiation from vegetation recorded at near and middle infrared wavelengths. For a boreal forest canopy, the relationship between VI3 and LAI was observed to be much stronger than that between NDVI and LAI. In addition, the LAI estimated using VI3 accounted for about 76% of the variation in field estimates of LAI, compared with about 46% when using the NDVI. We conclude that information provided by middle infrared radiation should be considered when estimating the leaf area index of boreal forest.

Keywords: LAI, middle infrared radiation, NDVI, remote sensing, VI3.

Introduction

One of the more promising methods for understanding ecosystem processes at regional to global scales (Curran and Foody 1994, Halliwell and Apps 1997) is the coupling of remotely sensed data with ecosystem process models (Asrar et al. 1984, Sellers et al. 1990, Wickland 1991). The remotely sensed data can provide accurate spatial estimates of 'driving' biophysical variables such as leaf area index (LAI). The evaluation of this methodology is integral to the BOREal Ecosystem-Atmosphere Study (BOREAS) program, which aims to develop and apply boreal ecosystem process models over regional scales (BOREAS Science Team 1993, Sellers et al. 1995).

Regional scale LAI can be estimated using data from coarse spatial resolution satellite sensors (Running 1990) such as the NOAA Advanced Very High Resolution Radiometer (AVHRR). This sensor measures radiation from the Earth's surface in five channels (Table 1), at a nominal spatial resolution of 1.21 km² across a swath width of 2700 km (Cracknell

1997) and LAI is linked causally with this radiation. These links include a negative relationship between LAI and visible radiation (range between 0.4 and 0.7 µm), due to absorption by leaf pigments and a positive relationship between LAI and near infrared (NIR) radiation (range between 0.7 and 1.5 µm), due to within-leaf scattering (Jensen 1983, Danson and Curran 1993). Both visible and NIR radiation data acquired by the AVHRR are commonly used in vegetation indices (e.g., the normalized difference vegetation index, NDVI = (NIR – visible)/(NIR + visible)). The strong positive relationship between LAI and NDVI, at least up to the reflectance asymptote of the canopy (Curran 1985), has been used to estimate and document the spatial and temporal variability of LAI (or a surrogate) for several forest ecosystems (Nemani and Running 1989, Foody and Curran 1994, Running et al. 1995, Fazakas and Nilsson 1996, Wellens 1997).

However, use of only visible and NIR radiation data does not fully exploit the information provided by the five measurement channels of the AVHRR (Table 1). For example, recent studies have revealed the importance for ecosystem study of Channel 3, which records middle infrared (MIR) radiation (range between 3.0 and 5.0 µm) (Laporte et al. 1995, Foody et al. 1996, Boyd and Ripple 1997, DeFries et al. 1997, Mantovani et al. 1997). Specifically, MIR radiation has been shown to provide more accurate estimates of biophysical properties such as LAI, and to be less affected by atmospheric or scan angle effects, than either visible or NIR radiation (Kaufman and Remer 1994, França and Setzer 1998).

Table 1. Spectral characteristics of the Advanced Very High Resolution Radiometer.

Channel number and name	Bandwidth (µm)
1. Visible	0.58–0.68
2. Near infrared	0.75–1.10
3. Middle infrared	3.55–3.93
4. Thermal infrared (1)	10.50–11.30
5. Thermal infrared (2) ¹	11.50–12.30

¹ The NOAA-6, -8, and -10 satellites have no Channel 5.

Unfortunately, regional scale estimation of LAI with MIR radiation may be unreliable (Kaufman and Remer 1994) because it comprises a mix of reflected and emitted components. At regional scales, the emitted radiation may be influenced more by confounding variables (e.g., localized atmospheric conditions, such as wind speed and air vapor conductance; or site-specific factors, such as topography and soil water conditions) than by biophysical properties related to LAI, such as basal area and tree density (Price 1989, Luvall et al. 1990, Nemani et al. 1993, Florinsky et al. 1994, Nichol 1995). It may be necessary, therefore, to remove emitted radiation from the total MIR radiation and use only the reflected component of MIR radiation (Kaufman and Remer 1994) for estimating LAI at and beyond the regional scale.

The reflected component of MIR radiation from a vegetation canopy is thought to be principally a function of the liquid water content of the canopy. An increase in LAI will be accompanied by an increase in the amount of canopy water, and thereby the ability of the canopy to absorb rather than reflect MIR radiation (Kaufman and Remer 1994). Studies comparing the NDVI response and canopy water amount for forest environments have noted a limited range in NDVI compared with canopy water amount (Roberts et al. 1997). Canopy structure, which is dependent on canopy depth and the area, orientation and distribution of leaves, is also believed to be an important, but secondary factor, determining the amount of shadow and thereby MIR radiation reflected from a canopy (Boyd and Curran 1998).

Reflected MIR radiation has been used in several studies (e.g., Shimabukuro et al. 1995), generally in combination with radiation data acquired at other wavelengths. The VI3 vegetation index combines information on canopy properties provided by NIR and MIR reflected radiation, and has been shown to estimate the biophysical properties of tropical forests more accurately than the NDVI (Boyd et al. 1999). The ability of the VI3 to estimate the LAI of boreal forests, with a natural LAI magnitude and range that is lower and narrower than that of tropical forests, is currently unknown. This research compared the accuracy of LAI estimates of boreal forest obtained by means of the NDVI and VI3 vegetation indices.

Materials and methods

Study area and data

This research focused on the Southern Study Area (SSA) of the BOREAS study region, situated on the southern edge of the Canadian boreal forest, 40 km north of Prince Albert, Saskatchewan. The SSA comprises approximately 10,000 km² of boreal forest (Sellers et al. 1995), dominated by jack pine (*Pinus banksiana* Lamb.) and aspen (*Populus tremuloides* Michx.) stands on the higher ground and black spruce (*Picea mariana* (Mill.) BSP) stands on the lower, poorly drained areas. The study area has an undulating topography, with altitudes between 550 and 730 m (Halliwell and Apps 1997).

As part of the BOREAS program, two independent data sets of estimated forest LAI (one-sided leaf area per unit ground

area) were obtained during late July–early August 1994. The first data set, collected by Plummer et al. (1995) with an LAI-2000 plant canopy analyzer and sunflecks ceptometer instruments (Li-Cor, Inc., Lincoln, NE), provided LAI estimates for nine sites across the SSA (hereafter referred to as LAI_{training} data). The second data set, collected concurrently by Chen et al. (1997) again with an LAI-2000 plant canopy analyzer (Li-Cor), provided further LAI estimates for 10 sites (hereafter referred to as LAI_{testing} data). In both cases, the LAI estimates for each site were made along transects 50 to 300 m long and were calibrated to allow comparison of the data sets with one another and with other LAI data sets (Chen and Cihlar 1995).

An NOAA-9 satellite AVHRR Local Area Coverage (LAC) image was acquired on July 21, 1994 and this coincided with the collection of LAI data. A mean forest LAI for each site was used in the subsequent analyses (Figure 1), and all of the LAI estimates along the transects at each site were assumed to fall within the area represented by an AVHRR pixel (Figures 2 and 3 show transect numbers per pixel).

Data processing and methods

The NOAA AVHRR image had undergone geometric pre-processing as part of the Canadian Centre for Remote Sensing's (CCRS) geocoding and compositing system (GEOCOMP) (Robertson et al. 1992, Cihlar and Teillet 1995) to correct for spacecraft orbit, altitude, and velocity, and Earth rotation and curvature. An AVHRR image subscene, covering the SSA, was registered to a geocoded (Friedal 1992) Landsat Thematic Mapper image based on 63 ground control points, with a registration accuracy (RMSE) of ± 0.59 of a pixel. This made it possible to locate on the image the sites where mean forest LAI had been estimated.

The top of atmosphere (TOA) radiances recorded by the AVHRR image in Channels 1 and 2 ($\text{W m}^{-2} \mu\text{m}^{-1} \text{sr}^{-1}$) were converted to TOA reflectance (Kidwell 1991) and used to derive NDVI for each AVHRR pixel covering the SSA. The reflected component of MIR radiation for each pixel covering the SSA was derived from TOA radiances in AVHRR Channels 3 and 4 ($\text{mW m}^{-2} \text{cm}^{-1} \text{sr}^{-1}$). Following the methodology of Kaufman and Remer (1994), the reflected component of MIR radiation was derived based on the assumption:

$$L_{3.75} = \rho_{3.75} + E_{3.75}, \quad (1)$$

where $L_{3.75}$ is total radiant energy measured in AVHRR Channel 3 (MIR radiation), $\rho_{3.75}$ is reflected energy (reflected component of AVHRR Channel 3) and $E_{3.75}$ is emitted energy (emitted component of AVHRR Channel 3). The reflected energy, $\rho_{3.75}$, hereafter referred to as MIR reflectance, was calculated with the assumption that energy emitted in the 10.5–11.3 μm spectral region (i.e., the brightness temperature calculated from the radiation in Channel 4) is related to $E_{3.75}$ through Planck's function. This information was used subsequently within:

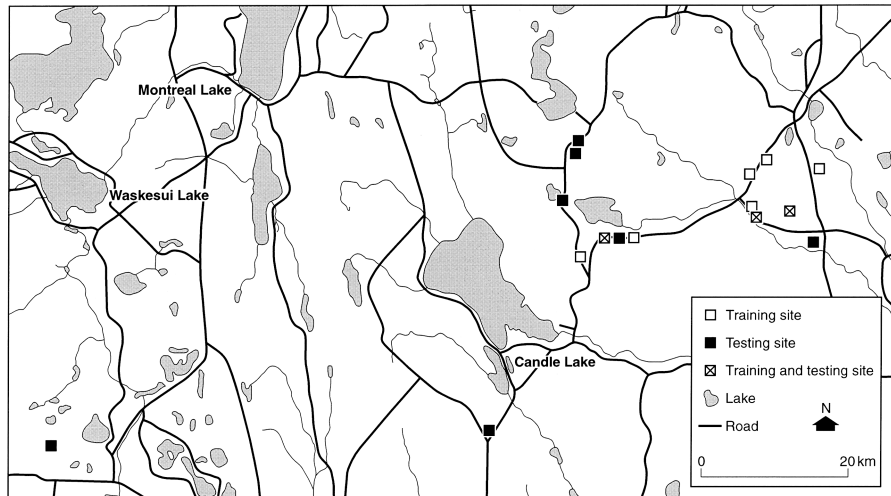


Figure 1. Map of the BOREAS SSA, showing the sites for which LAI was estimated. Note, training sites are those where Plummer et al. (1995) collected data and testing sites those areas where Chen et al. (1997) collected data.

$$\rho_{3.75} = \frac{L_{3.75} - t_{3.75} \epsilon_{3.75} B_{3.75}(T)}{t'_{3.75} \frac{F_0 \mu_0}{\pi} - t_{3.75} \epsilon_{3.75} B_{3.75}(T)}, \quad (2)$$

where $B_{3.75}$ is the Planck function in AVHRR Channel 3, F_0 is the incident solar radiance at TOA in AVHRR Channel 3, μ_0 is the cosine of the solar zenith angle, $\epsilon_{3.75}$ is the emissivity of the target in AVHRR Channel 3, and $t_{3.75}$ and $t'_{3.75}$ are the one- and two-way atmospheric transmission of radiation in AVHRR Channel 3, respectively. Transmissivities were assumed to be of the mid-latitude atmosphere type and constant across the SSA (Kaufman and Remer 1994). The emissivity was assumed to be 0.98, the value for spherical canopies at an LAI of approximately 2 (Guoquan and Zhengzhi 1992, Olioso 1995). The MIR reflectance value for each pixel was used with NIR reflectance to derive the VI3 index (Kaufman and Remer

1994):

$$VI3 = \frac{\text{NIR reflectance} - \text{MIR reflectance}}{\text{NIR reflectance} + \text{MIR reflectance}}. \quad (3)$$

The outcome of data processing was two vegetation index images of the SSA for comparison with the LAI data.

Results and discussion

The LAI_{training} data were used to develop predictive regression relationships between LAI and NDVI (Figure 2) and LAI and VI3 (Figure 3). Despite their small sample size ($n = 9$), these relationships agree with those observed in previous studies (Boyd et al. 1999), where the negative relationship between LAI and VI3 ($r^2 = 0.62$) was stronger than the relationship be-

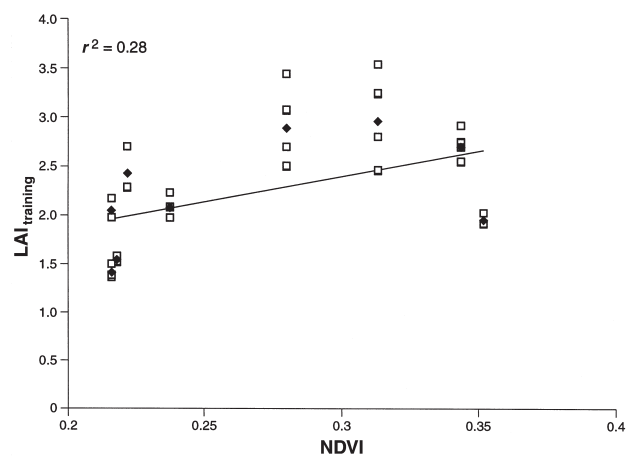


Figure 2. Predictive relationship between NDVI and LAI estimates recorded by Plummer et al. (1995) ($LAI = 0.82 + 5.24NDVI$). For illustrative purposes, the LAI estimates for each transect are shown (\square). The regression was developed for a mean LAI estimate for each site (\blacklozenge) because all transects were assumed to fall into the area covered by an AVHRR pixel.

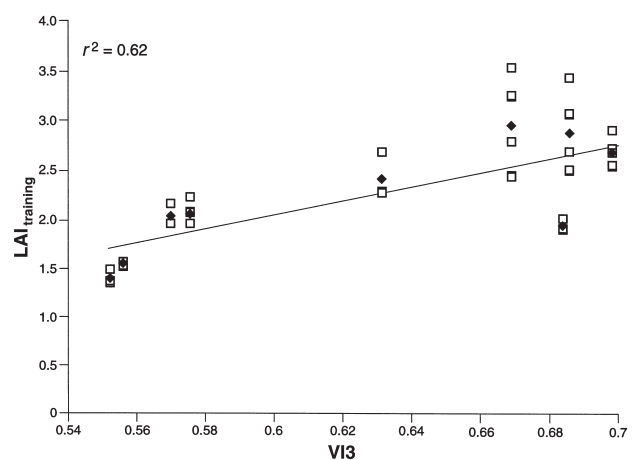


Figure 3. Predictive relationship between VI3 and LAI estimates recorded by Plummer et al. (1995) ($LAI = -2.3 + 7.24VI3$). For illustrative purposes, the LAI estimates for each transect are shown (\square). The regression was developed for a mean LAI estimate for each site (\blacklozenge) because all transects were assumed to fall into the area covered by an AVHRR pixel.

tween LAI and NDVI ($r^2 = 0.28$). This demonstrates the sensitivity of the VI3 index to boreal forest LAI. Because both vegetation indices used NIR reflectance in the same fashion, the replacement of visible reflectance with MIR reflectance in VI3 accounted for the stronger relationship between LAI and VI3.

The scatter exhibited in both these relationships can be attributed to (i) the limited range of LAI in boreal forest, (ii) the asymptotic nature of the relationships, (iii) variability in the reflectance of understory vegetation, and (iv) atmospheric attenuation. The first three factors have similar effects on both vegetation indices. This is the case even for (iii), where the low solar angle and resultant shadow mask the effect of variability in understory vegetation at all wavelengths. However, atmospheric scattering is much greater in visible than in MIR wavelengths. Replacing the visible reflectance component of the NDVI with MIR reflectance in VI3 reduces atmospheric attenuation effects. Furthermore, water content of leaves within a canopy is usually less variable than chlorophyll content (Malthus et al. 1993). Consequently, the scatter in the relationship between remotely sensed data and LAI would be reduced if VI3 were used instead of the NDVI.

The predictive regression relationships developed in Figures 2 and 3 were applied to both the NDVI and VI3 images and provided remotely sensed estimates of LAI for those sites for which LAI_{testing} data were available (Figure 4). The coefficients of determination (r^2) derived for the relationships between LAI_{testing} and LAI estimated by the NDVI and VI3, were 0.46 and 0.76, respectively (significantly different at 95% confidence level; $P = 0.1$). These findings suggest that the NDVI

is considerably less accurate than VI3 for estimating LAI of boreal forest.

This study demonstrates the value of remotely sensed radiation reflected at MIR wavelengths. However, there are three issues that require attention before these data can be used at regional to global scales. First, research exploring the use of MIR reflectance for LAI estimation has focused on only a limited number of biomes, therefore, this work needs extending to other biomes differing in LAI magnitude and range, canopy structure, soil type and understory composition. Second, remote sensing for ecosystem process research at regional to global scales requires the ability to monitor over time and scale-up between images acquired at different spatial resolutions (Cihlar et al. 1997). However, relative to the radiation data acquired in visible and NIR wavelengths, understanding of the interaction of MIR reflectance with vegetation is poor; little is known of temporal variability and effects of the growing season on the MIR radiation from a canopy. Further, the MIR channel of the NOAA AVHRR sensor is currently not complementary to that of other sensors differing in spatial resolution (e.g., SPOT HRV, Landsat TM). Third, the method for deriving MIR reflectance from total radiant energy measured in AVHRR Channel 3 is still evolving, and is dependent on several assumptions (e.g., emissivity) (Nerry et al. 1998, Roger and Vermote 1998). Once these issues are resolved, the use of MIR reflectance may increase the accuracy with which the LAI of ecosystems can be estimated. Such optimization of remotely sensed data, acquired by a number of sensors operating currently (e.g., NOAA AVHRR, ERS ATSR, Terra MODIS), and in the future (e.g., Envisat AATSR), has wide implications for regional to global scale modeling of ecosystem function.

We conclude that the VI3 vegetation index provides more accurate estimates of boreal forest LAI than the NDVI. The inclusion of information provided by MIR reflectance enhanced the accuracy of LAI estimates and its subsequent use should be considered.

Acknowledgments

This paper was written while TEW held an internship at the Canadian Forest Service, Québec City. The work was funded by the Natural Environment Research Council (Research Studentship GT96/273/EO to TEW). The research follows on from the BOREAS project, within which we collectively acknowledge all individuals and agencies.

References

- Asrar, G., M. Fuchs, E.T. Kanemasu and J.L. Hatfield. 1984. Estimating absorbed photosynthetic radiation and leaf area index from spectral reflectance in wheat. *Agron. J.* 76:300–306.
- BOREAS Science Team. 1993. Boreal Ecosystem–Atmosphere Study, Experiment Plan. Version 1, NASA/GSFC, Greenbelt, MD, 370 p.
- Boyd, D.S. and W.J. Ripple. 1997. Potential vegetation indices for determining global forest cover. *Int. J. Remote Sens.* 18: 1395–1401.

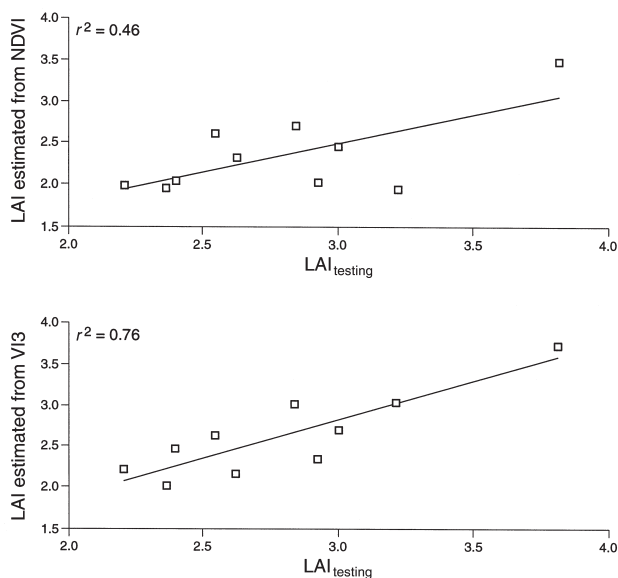


Figure 4. Relationships between the LAI estimated by Chen et al. (1997) and LAI estimated by NDVI and VI3. The remotely sensed LAI was derived by applying the predictive regression relationships developed in Figures 2 and 3 to the NDVI and VI3 images and LAI extracted for those pixels that corresponded to the sites for which LAI had been estimated in the field.

- Boyd, D.S. and P.J. Curran. 1998. Using remote sensing to reduce uncertainties in the global carbon budget: the potential of radiation acquired in middle infrared wavelengths. *Remote Sens. Rev.* 16: 293–327.
- Boyd, D.S., G.M. Foody and P.J. Curran. 1999. The relationship between the biomass of Cameroonian tropical forests and radiation reflected in middle infrared wavelengths (3.0–5.0 μm). *Int. J. Remote Sens.* 20:912–920.
- Chen, J.M. and J. Cihlar. 1995. Quantifying the effect of canopy architecture on optical measurements of leaf area index using two gap size analysis methods. *IEEE Trans. Geosci. Remote Sens.* 33:777–787.
- Chen, J.M., P.M. Rich, S.T. Gower, J.M. Norman and S. Plummer. 1997. Leaf area index of boreal forests: theory, techniques and measurements. *J. Geophys. Res.* 102:429–443.
- Cihlar, J. and P.M. Teillet. 1997. Forward piecewise linear model for quasi-real time processing of AVHRR data. *Can. J. Remote Sens.* 21:22–27.
- Cihlar, J., J. Chen and Z. Li. 1997. Seasonal AVHRR multichannel data sets and products for studies of surface-atmosphere interactions. *J. Geophys. Res.* 102:625–629.
- Curran, P.J. 1985. Principles of remote sensing. Harlow, London, 285 p.
- Curran, P.J. and G.M. Foody. 1994. Environmental issues at regional to global scales. In *Environmental Remote Sensing from Regional to Global Scales*. Eds. Curran, P.J. and G.M. Foody. John Wiley, Chichester, pp 1–7.
- Cracknell, A.P. 1997. AVHRR: The Advanced Very High Resolution Radiometer. Taylor and Francis, London, 534 p.
- Danson, F.M. and P.J. Curran. 1993. Factors affecting the remotely sensed response of coniferous forest plantations. *Remote Sens. Environ.* 43:55–65.
- DeFries, R., M. Hansen, M. Steininger, R. Dubayah, R. Sohlberg and J. Townshend. 1997. Subpixel forest cover in central Africa from multisensor, multitemporal data. *Remote Sens. Environ.* 60:228–246.
- Fazakas, Z. and M. Nilsson. 1996. Volume and forest cover estimation over southern Sweden using AVHRR data calibrated with TM data. *Int. J. Remote Sens.* 17:1701–1709.
- Florinsky, I.V., T.B. Kulagina and J.L. Meshalkina. 1994. Influence of topography on landscape radiation temperature distribution. *Int. J. Remote Sens.* 15:3147–3153.
- Foody, G.M. and P.J. Curran. 1994. Estimation of tropical forest extent and regenerative stage using remotely sensed data. *J. Biogeogr.* 21:223–244.
- Foody, G.M., D.S. Boyd and P.J. Curran. 1996. Relations between tropical forest biophysical properties and data acquired in AVHRR channels 1–5. *Int. J. Remote Sens.* 17:1341–1355.
- França, H. and A.W. Setzer. 1998. AVHRR temporal analysis of a savanna site in Brazil. *Int. J. Remote Sens.* 19:3127–3140.
- Friedal, J. 1992. System description of the Geocoded Image Correction System. Report GC-MA-50-3915. MacDonald Detwiller, Richmond, Canada, 186 p.
- Guoquan, D. and L. Zhengzhi. 1992. The apparent emissivity of vegetation canopies. *Int. J. Remote Sens.* 14:183–188.
- Halliwell, D.H. and M.J. Apps. 1997. BOREal Ecosystem Atmosphere Study (BOREAS) biometry and auxiliary sites: locations and descriptions. Natural Resources Canada, Alberta, 254 p.
- Jensen, J.R. 1983. Biophysical remote sensing. *Ann. Assoc. Am. Geogr.* 73:111–132.
- Kaufman, Y.J. and L.A. Remer. 1994. Detection of forests using MID-IR reflectance, an application for aerosol studies. *IEEE Trans. Geosci. Remote Sens.* 32:672–683.
- Kidwell, K.B. 1991. NOAA Polar Orbiter Data TIROS-N, NOAA-6, NOAA-7, NOAA-8, NOAA-9, NOAA-10, NOAA-11 and NOAA-12. Users Guide. NASA, Washington, D.C., 293 p.
- Laporte, N., C. Justice and J. Kendall. 1995. Mapping the dense humid forest of Cameroon and Zaire using AVHRR satellite data. *Int. J. Remote Sens.* 16:1127–1145.
- Luvall, J.C., D. Lieberman, M. Lieberman, G.S. Hartshorn and R. Peralta. 1990. Estimation of tropical forest canopy temperature, thermal response number, and evapotranspiration using an aircraft-based thermal sensor. *Photogramm. Eng. Remote Sens.* 56:1393–1401.
- Malthus, T.J., B. Andrieu, F.M. Danson, K.W. Jaggard and M.D. Steven. 1993. Candidate high spectral resolution infrared indices for crop cover. *Remote Sens. Environ.* 46:204–212.
- Mantovani, A.C.D.M. and A.W. Setzer. 1997. Deforestation detection in the Amazon. *Int. J. Remote Sens.* 18:319–333.
- Nemani, R.R. and S.W. Running. 1989. Estimation of regional surface evapotranspiration from NDVI and thermal IR AVHRR data. *J. Appl. Meteorol.* 28:276–284.
- Nemani, R.R., L. Pierce, S. Running and S. Goward. 1993. Developing satellite-derived estimates of surface moisture status. *J. Appl. Meteorol.* 32:548–557.
- Nerry, F., F. Petitcolin and M.P. Stoll. 1998. Bidirectional reflectivity in AVHRR channel 3: application to a region in northern Africa. *Remote Sens. Environ.* 66:298–316.
- Nichol, J.E. 1995. Monitoring tropical rain forest microclimate. *Photogramm. Eng. Remote Sens.* 61:1159–1165.
- Olioso, A. 1995. Simulating the relationship between thermal emissivity and the Normalised Difference Vegetation Index. *Int. J. Remote Sens.* 16:3211–3216.
- Plummer, S.E. and N.S. Lucas. 1995. Report of the BOREAS Intensive Field Campaign 1994. Remote Sensing Applications Development Unit Report No. 95/5. British National Space Centre, Monks Wood, Huntingdon, 12 p.
- Price, J.C. 1989. Quantitative aspects of remote sensing in the thermal infrared. In *Theory and Applications of Optical Remote Sensing*. Ed. G. Asrar. John Wiley, New York, pp 578–603.
- Roberts, D.A., R.O. Green and J.B. Adams. 1997. Temporal and spatial patterns in vegetation and atmospheric properties from AVIRIS. *Remote Sens. Environ.* 62:223–240.
- Robertson, B., A. Erickson, J. Friedel, B. Guindon, T. Fisher, R. Brown, P. Teillet, M. D'Iorio, J. Cihlar and A. Sencz. 1992. GEOCOMP, a NOAA AVHRR geocoding and compositing system. *Proc. Int. Soc. Photogrammetry and Remote Sensing Conference. ISPRS*, Washington, DC, pp 223–228.
- Roger, J.C. and E.F. Vermote. 1998. A method to retrieve the reflectivity signature at 3.75 μm from AVHRR data. *Remote Sens. Environ.* 64:103–114.
- Running, S.W. 1990. Estimating terrestrial primary productivity by combining remote sensing and ecosystem simulation. In *Remote Sensing of Biosphere Function*. Eds. R.J. Hobbs and H.A. Mooney. Springer-Verlag, New York, pp. 65–86.
- Running, S.W., T.R. Loveland, L.L. Pierce, R.R. Nemani and E.R. Hunt. 1995. A remote sensing based vegetation logic for global land cover analysis. *Remote Sens. Environ.* 51:39–48.
- Sellers, P.J., F.G. Hall, D.E. Strebel, G. Asrar and R.E. Murphy. 1990. Satellite remote sensing and field experiments. In *Remote Sensing of Biosphere Function*. Eds. Hobbs, R.J. and H.A. Mooney. Springer-Verlag, New York, pp. 169–201.
- Sellers, P.J., F.G. Hall, H. Margolis, B. Kelly, D. Baldocchi, G. den Hartog, J. Cihlar, M.G. Ryan, B. Goodison, P. Crill, K.J. Ranson, D. Lettenmaier and D.E. Wickland. 1995. The BOREal Ecosystem Atmosphere Study (BOREAS): an overview and early results from

- the 1994 field year. *Bull. Am. Meteorol. Soc.* 76:1549–1577.
- Shimabukuro, Y.E., B.N. Holben and C.J. Tucker. 1994. Fraction images derived from NOAA AVHRR data for studying the deforestation in the Brazilian Amazon. *Int. J. Remote Sens.* 15:517–520.
- Wellens, J. 1997. Rangeland vegetation dynamics and moisture availability in Tunisia: an investigation using satellite and meteorological data. *J. Biogeogr.* 24:845–855.
- Wickland, D.E. 1991. Global ecology: the role of remote sensing. *In* *Modern Ecology: Basic and Applied Aspects*. Eds. G. Esser and D. Overdieck. Elsevier, Amsterdam, pp 725–750.